PERSPECTIVE PROJECTIONS IN THE SPACE-FREQUENCY PLANE AND FRACTIONAL FOURIER TRANSFORMS

İ. Şamil Yetik, Haldun M. Ozaktas, Billur Barshan, Levent Onural

Bilkent University, Department of Electrical Engineering,
TR-06533 Bilkent, Ankara, Turkey

ABSTRACT

We analyse perspective projections in the space-frequency plane and show that under certain conditions they can be approximately modelled in terms of the fractional Fourier transform. The region of validity of the approximation is examined. Numerical examples are presented.

1. INTRODUCTION

Perspective projections are used in many applications in image and video processing, especially when confronted with natural or artificial scenes with depth (for instance, in robot vision applications). Perspective projection can be considered as a geometric or pointwise transformation, in the sense that each point of the input is mapped to another point in the output [1, 2]. In this paper we will examine the perspective projection in the space-frequency plane and show that its effect on the input can be modelled in terms of the fractional Fourier transform.

A widely employed space-frequency representation is the Wigner distribution is going to be used in this paper. The Wigner distribution provides information regarding the distribution of the signal energy over space and frequency. A discussion and properties of the Wigner distribution may be found in [3].

The fractional Fourier transform is a generalization of the ordinary Fourier transform with a fractional order parameter a. It has found many applications in optics and signal processing [4-9]. We refer the reader to [4] for a comprehensive treatment and further references, and to [6] for a shorter introduction. The zeroth order fractional Fourier transform corresponds to the identity operation and the first order fractional Fourier transform corresponds to the ordinary Fourier transform. Furthermore, the fractional Fourier transform is index additive; that is, the a_1th order fractional Fourier transform of the a_2th order fractional Fourier transform is equal to the $(a_1 + a_2)$th order fractional Fourier transform. The ath order fractional Fourier transform corresponds to a clockwise rotation of the Wigner distribution by an angle $\alpha = a\pi/2$ in the space-frequency plane: The fractional Fourier transform has a fast implementation with compexity $O(N \log N)$ [4, 6].

To understand why the fractional Fourier transform is expected to play a role in perspective projections, let us consider the perspective projection of an image exhibiting periodic features, such as a railroad track. More "distant" parts of the image will appear in the projection smaller than "closer" parts. Thus a periodic or harmonic feature of certain frequency will be mapped such that it exhibits a monotonic increasing frequency. Under certain conditions, this increase can be assumed linear so that the harmonic function is mapped to a chirp function. Since fractional Fourier transforms are known to map harmonic functions to chirp functions, we expect that perspective projections can be modelled in terms of fractional Fourier transforms. The purpose of this paper is to formulate this relationship.

In the next section we are going to present the perspective model we use and examine the effect of the perspective projection on the Wigner distribution. In the following section, we will discuss the relation between the fractional Fourier transform and perspective projections based on their effects on the Wigner distribution. We will discuss how perspective projections can be modelled as shifted and fractional Fourier transformation. The last section is devoted to an analysis of the errors and the region of validity of the approximations.

2. PERSPECTIVE TRANSFORMATION

The perspective model we use is shown in figure 1. Initially we consider perspective projections for one-dimensional signals, since this significantly simplifies the presentation. The horizontal axis, labeled x, represents the original object space. The vertical axis, labeled x_p, represents the perspective projection space. The point A with coordinates $(-x_0, x_{po})$ is the perspective center or the focus point. We denote the original signal (object) by $f(x)$ and its perspective projection by $g(x_p)$. We assume that most of the energy of $f(x)$ is confined to the interval $[\bar{x} - \Delta x/2, \bar{x} + \Delta x/2]$. In the frequency domain, we assume that most of the energy of $F(\sigma_x)$, the Fourier transform of $f(x)$, is confined to the interval $[\bar{\sigma}_x - \Delta\sigma_x/2, \bar{\sigma_x} + \Delta\sigma_x/2]$. The value of $f(x)$ at each x is mapped to the point x_p, which is the projection of the point x:

$$x_p = \frac{x x_{po}}{x + x_0}, \tag{1}$$

$$x = \frac{x_0 x_p}{x_{po} - x_p}, \tag{2}$$

which can be derived by simple geometry. Thus, the projection $g(x_p)$ is expressed as follows:

$$g(x_p) = f\left(\frac{x_0 x_p}{x_{po} - x_p}\right). \tag{3}$$

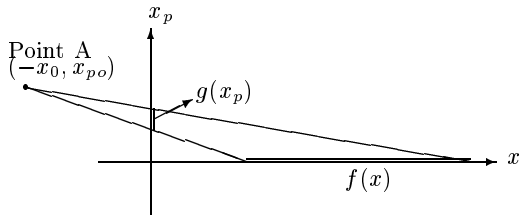

Figure 1: Perspective model: $f(x)$ represents the input distribution on the x axis, $g(x_p)$ represents its perspective projection onto the x_p axis. The point A with coordinates $(-x_0, x_{po})$ is the perspective center or the focus point.

The interval to which most of the energy of $g(x_p)$ is approximately confined can be determined using 1.

In order to see the effect of perspective projections in the space-frequency plane, we decompose $f(x)$ into harmonics as follows:

$$f(x) = \int F(\sigma_x) \exp[i2\pi x\sigma_x]\, d\sigma_x. \tag{4}$$

where $F(\sigma_x)$ is the Fourier transform of $f(x)$. Using (3) and linearity we obtain the following expression for $g(x_p)$:

$$g(x_p) = \int F(\sigma_x) h(x_p, \sigma_x)\, d\sigma_x, \tag{5}$$

where

$$h(x_p, \sigma_x) = \exp\left[i2\pi\sigma_x \left(\frac{x_0 x_p}{x_{po} - x_p}\right)\right] d\sigma_x. \tag{6}$$

We will initially concentrate on a single exponential with frequency $\bar{\sigma}_x$ and study the effect of perspective projection in the space-frequency plane. Then, we will construct $g(x_p)$ by first decomposing $f(x)$ in terms of exponentials and using (5).

The Wigner distribution of $h(x_p, \bar{\sigma}_x)$ cannot be explicitly obtained. Therefore, to continue our analytical development, we expand the phase of $h(x_p, \bar{\sigma}_x)$ in a Taylor series. We will expand the phase of $h(x_p, \bar{\sigma}_x)$ around the point which $\bar{x}$ is mapped to:

$$\frac{\bar{x}}{\bar{x} + x_0} x_{po} \tag{7}$$

which we express as κx_{po} where $\kappa = \frac{\bar{x}}{\bar{x}+x_0}$. Expanding the phase of $h(x_p, \bar{\sigma}_x)$ around κx_{po} we obtain the following after some algebra:

$$h(x_p, \bar{\sigma}_x) = \exp\left[i2\pi\sigma_x x_0 \left(\frac{x_p^2}{(1-\kappa)^3 x_{po}^2} + \frac{x_p(1-3\kappa)}{(1-\kappa)^3 x_{po}} + \frac{\kappa^3}{(1-\kappa)^3} + \ldots\right)\right]. \tag{8}$$

Ignoring terms higher than the second order, the projection of a harmonic is seen to be a chirp function. The validity of this approximation requires the third order term to be much smaller than the second order term:

$$|\kappa + 2| \ll |2x_{po}(\kappa - 1)|. \tag{9}$$

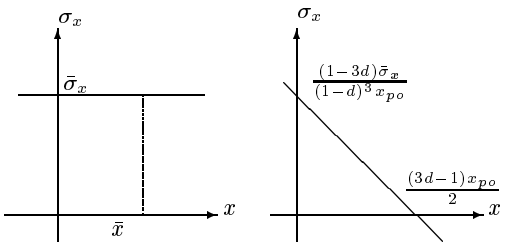

Figure 2: (a) Wigner distribution of the original exponential. (b) Wigner distribution of the approximate perspective projection: a chirp.

This approximation is more accurate for larger values of x_{po}. This is expected since larger x_{po} correspond to less deep perspective projections. The Wigner distribution of the chirp given in (8) is a line delta given by

$$\delta\left(\sigma_x + \frac{2\bar{\sigma}_x}{(1-\kappa)^3 x_{po}^2} x_p + \frac{\bar{\sigma}_x(1-3\kappa)}{(1-\kappa)^3 x_{po}}\right), \tag{10}$$

and is shown in figure 2b.

Having obtained an approximate analytical form for the perspective projection of a harmonic, as well as its Wigner distribution, we now move on to our discussion of perspective projections in the space-frequency plane, as well as its relation to the fractional Fourier transform.

3. RELATION BETWEEN PERSPECTIVE TRANSFORMATION AND FRACTIONAL FOURIER TRANSFORM

In the previous section we obtained an approximate expression for the Wigner distribution of the perspective projection of a single exponential. The Wigner distribution of a typical exponential and the Wigner distribution of the approximate perspective projection of the exponential are shown in figure 2. The angle the line delta makes with the x axis is $\arctan\left(\frac{2\bar{\sigma}_x}{(1-d)^3 x_{po}^2}\right)$, which depends on $\bar{\sigma}_x$. The fact that the oblique line delta is a rotated version of the horizontal line delta suggests a role for the fractional Fourier transform since this operation corresponds to rotation in the space-frequency plane.

We will now show how the perspective projection of a signal can be approximately expressed in terms of the fractional Fourier transform. We claim that the perspective projection of a signal can be obtained from, or modelled by, the following steps:

1. Shift the signal by $\bar{x}$ in the negative x direction and by $\bar{\sigma}_x$ in the negative σ_x direction. This translates the Wigner distribution of the signal to the origin of the space-frequency plane.
2. Take the fractional Fourier transform with the order $a = \frac{-2}{\pi} \arctan\left(\frac{2\bar{\sigma}_x(\bar{x}+x_0)^3}{x_{po}^2 x_0^2}\right)$. This rotates the Wigner distribution by an angle $a\pi/2$.
3. Shift the result by $\frac{\bar{x}x_{po}}{\bar{x}+x_0}$ in the positive x direction and by $\frac{\bar{\sigma}_x(\bar{x}+x_0)^2}{x_0 x_{po}}$ in the positive σ_x direction.

These steps represent a decomposition of the overall effect of the perspective projection, from which we see that the substance of perspective projection is essentially to effect a rotation in the space-frequency plane. However, this rotation is enacted on the space-frequency content of the signal referred to the origin of the space-frequency plane.

Different frequency components of the signal require different fractional Fourier orders, because the order a given in step 3 depends on $\bar{\sigma}_x$. However, as we will see, under certain conditions, a satisfactory approximation can be obtained by using a uniform order corresponding to the central frequency of the signal.

We now demonstrate our claim that perspective projection can be decomposed into the three steps given above. We start by decomposing $f(x)$ into harmonics:

$$f(x) = \int F(\sigma_x) \exp[2i\pi x\sigma_x]\, d\sigma_x, \tag{11}$$

We will concentrate on a single harmonic component $\exp[i2\pi x\sigma_x]$ and the result for general $f(x)$ will follow by linearity. Applying step 1 to a single harmonic we obtain

$$\exp[i2\pi\bar{x}\sigma_x]. \tag{12}$$

Now, we apply step 2 and step 3 to this result to obtain

$$\sqrt{1+i\frac{2\sigma_x\bar{x}+x_0}{x_{po}^2x_0^3}}\exp[i2\pi\bar{x}\sigma_x]\times\exp\left[\left(i2\pi x^2\sigma_x\frac{\bar{x}+x_0}{x_{po}^2x_0^3}\right)\right] \tag{13}$$

Finally, we apply step 4 and obtain our final result:

$$\begin{aligned}&\sqrt{1+i\frac{2\sigma_x(\bar{x}+x_0)^3}{x_{po}^2x_0^3}}\exp[i2\pi\bar{x}\sigma_x]\\ &\times\exp\left[i2\pi\sigma_x\left(x-\frac{\bar{x}x_{po}}{\bar{x}+x_0}\right)^2\left(\frac{\bar{x}+x_0}{x_{po}^2x_0^3}\right)\right]\\ &\times\exp\left[i4\pi\sigma_x\left(\frac{\bar{x}+x_0^2}{x_0^2x_{po}}\right)\right].\end{aligned} \tag{14}$$

Multiplying this with $F(\sigma_x)$ and integrating over σ_x yields the desired approximate expression for the perspective projection of $f(x)$, which is the mathematical expression of the four steps outlined above.

To see that this expression is indeed an approximation of the perspective projection, we again concentrate on a single harmonic component whose exact perspective projection is

$$\exp\left[2i\pi\sigma_x\frac{x_0x_p}{x_{po}-x_p}\right] \tag{15}$$

Using the taylor series expansion we obtain

$$\exp\left[i2\pi\sigma_x x_0\left(\frac{x_p^2}{(1-\kappa)^3x_{po}^2}+\frac{x_p(1-3\kappa)}{(1-\kappa)^3x_{po}}+\frac{\kappa^3}{(1-\kappa)^3}\right)\right], \tag{16}$$

which we see differs from (14) only by a constant factor. As far as a single harmonic component is concerned, the only approximation that is involved is the binomial expansion in the exponent. When the harmonic components are superposed to obtain the original function $f(x)$, we make the additional approximation of using the order corresponding to the center frequency for all harmonic components. Thus our three-step procedure will deviate from the exact perspective projection more and more as the bandwidth of $f(x)$ is increased. The limitations associated with this approximation will be discussed in the next section.

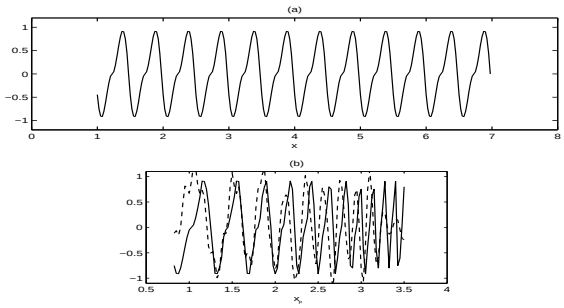

Figure 3: a) Original signal. b) Exact perspective projection superimposed with the fractional Fourier approximation.

As an example we consider the narrowband signal shown in figure 3. Again, the exact perspective projection and the fractional Fourier approximation are superimposed in part b of the same figure. We observe that the approximation is quite satisfactory except very near the edges, which should be avoided.

4. ERROR ANALYSIS

In this section we examine the conditions under which the fractional Fourier transform approximation to the perspective projection is valid. We first examine the modifications the Wigner distribution undergoes corresponding to the approximation. Since we know that the approximation can be decomposed into the four steps given in section 3, it is an easy matter to find the resulting changes in the Wigner distribution. To estimate the error inherent in our approximation, we will think of the original Wigner distribution to consist of horizontal strips of narrow frequency components. The major approximation we make is to replace the fractional orders required by these different frequency components by a single order corresponding to the central frequency. To determine the error introduced by this approximation, we will determine how the highest and lowest frequency strips would be mapped had their individual frequencies been used instead of the center frequency. Let us assume that most of the energy of the Wigner distribution of a signal is concentrated in a rectangular region in the space-frequency plane (figure 4a). Part b of the same figure shows the Wigner distribution corresponding to the fractional Fourier approximation (solid lines). The dashed lines, on the other hand, show the Wigner contour obtained by using the individual frequencies for the highest and lowest frequency strips.

Our error criteria will be the deviations of the corners of the two superimposed Wigner contours in figure 4b. There will be one spatial deviation and one frequency deviation for each of the four corners of the contours. We will normalize

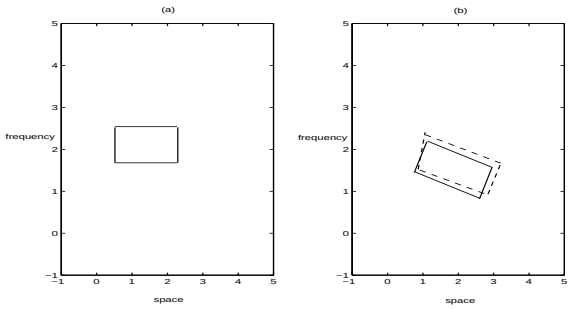

Figure 4: (a) Wigner distribution of the original signal. (b) Comparison of Wigner distributions underlying error analysis.

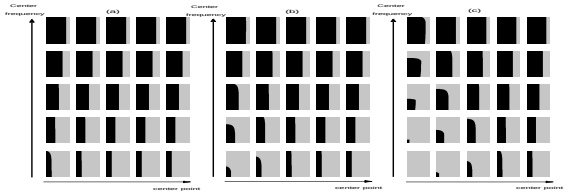

Figure 5: The dark regions represent the parameter combinations whose normalized error is less than 10%. See text for explanation.

the spatial deviation by Δx and the frequency deviations by $\Delta\sigma_x$ and take the maximum of the resulting eight normalized deviations as our final error measure. Expression for the eight normalized deviations can be derived easily.

It does not seem possible to analytically derive conclusions using these formulae so that we will resort to numerically obtained plots. The approximation will be assumed to be acceptable if the maximum normalized error is less than 10%. The error criteria we use give the error as a function of six variables: $x_0, x_{po}, \bar{x}, \bar{\sigma}_x, \Delta x, \Delta\sigma_x$. However, normalizing all variables by x_0, the number of variables can be reduced to five. Figure 5 shows the region where the maximum normalized error is less than 10% as darker regions, whereas the lighter regions are where the error is large. The horizontal axis in each of the 75 plots represents the value of $\Delta x/x_0$ and the vertical axis represents $\Delta\sigma_x/x_0$. Both of these variables range from $10^{1/30}$ to $10^{100/30}$ in these log-log plots.

.

Each member of the 5×5 matrices of plots corresponds to different values of $\bar{x}/x_0$ (horizontal) $\bar{\sigma}_x/x_0$ (vertical). The five seperate values of $\bar{x}/x_0$ are
$10^{-1/2}, 10^{0/2}, 10^{1/2}, 10^{2/2}, 10^{3/2}$ and the five seperate values of $\bar{\sigma}_x/x_0$ are
$10^{-1/2}, 10^{0/2}, 10^{1/2}, 10^{2/2}, 10^{3/2}$. The three groups of 25 plots each correspond to different values of the perspective point. Figure 5a: $x_{po}/x_0 = 0.1$, figure 5b: $x_{po}/x_0 = 1$, Figure 5c: $x_{po}/x_0 = 10$.

This set of plots covering a broad range of the parameter values allows us to determine whether the approximation developed is acceptable for a certain range of parameters. Generally speaking, we have larger acceptable regions for larger values of $\bar{\sigma}_x$. Unsurprisingly, the approximation is strained as Δx and $\Delta\sigma_x$ increase, i.e. as the space-bandwidth product of the signal increases.

5. CONCLUSION

In this paper we examined perspective transformations in the space-frequency plane and showed how to approximate the perspective projection in terms of the fractional Fourier transform. Our main motivation was that the fractional Fourier transform approximately captures the essence of the warping characteristic of perspective transformations. We observed that perspective projection approximately maps harmonic components into chirps and therefore can be modelled in terms of the fractional Fourier transform. We saw that the substance of perspective projection is essentially to effect a rotation in the space-frequency plane. However, this rotation is enacted on the space-frequency content of the signal referred to the origin of the space-frequency plane. Elementary numerical examples for both one-dimensional signals and two-dimensional images are presented. The errors associated with the approximation and the region of validity with respect to the approximations involved are numerically discussed.

REFERENCES

[1] D. Vernon. Machine vision: Automated visual inspection and robot vision. Prentice Hall New York, 1991.

[2] A. Low. Introductory computer vision and image processing. McGraw-Hill New York, 1991.

[3] L. Cohen. Time-frequency analysis. Prentice Hall PTR, Englewood Cliffs, New Jersey, 1995.

[4] H. M. Ozaktas, D. Mendlovic, M. A. Kutay and Z. Zalevsky. The fractional Fourier transform and time-frequency representations. John Wiley and Sons, 2000.

[5] H. M. Ozaktas, B. Barshan, D. Mendlovic, and L. Onural. Convolution, filtering, and multiplexing in fractional Fourier domains and their relation to chirp and wavelet transforms. *J. Opt. Soc. Am. A* 11:547–559, 1994.

[6] H. M. Ozaktas, M. A. Kutay and D. Mendlovic. Introduction to the fractional Fourier transform and its applications. in: P. W. Hawkes, ed., *Advances in Imaging and Electron Physics.* Academic Press, San Diego, California, 1998, pp. 239-291.

[7] M. F. Erden, M. A. Kutay, and H. M. Ozaktas. Repeated filtering in consecutive fractional Fourier domains and its application to signal restoration. *IEEE Trans Signal Processing*, 47:1458–1462, 1999.

[8] D. Mendlovic, Z. Zalevsky, A. W. Lohmann, and R. G. Dorsch. Signal spatial-filtering using the localized fractional Fourier transform. *Opt Commun*, 126:14–18, 1996.

[9] V. Namias. The fractional order Fourier transform and its application to quantum mechanics. *J Inst Maths Applics*, 25:241–265, 1980.